

Unoccupied states on Pd(110) and the surface potential barrier

N. V. Smith and C. T. Chen

AT&T Bell Laboratories, Murray Hill, New Jersey 07974-2070

J. M. Tranquada and P. D. Johnson

Department of Physics, Brookhaven National Laboratory, Upton, New York 11973-5000

(Received 17 June 1988)

Inverse photoemission spectra on Pd(110) reveal bulk band-structure features, and surface-state features in the projected gaps centered at points \bar{Y} and \bar{X} . The energy dispersion of the bulk band-structure features is in agreement with direct-transition predictions. Surface-state energies and their dispersion are reproduced with a nearly-free-electron model and a surface-barrier model which places the image plane 2.3 a.u. beyond the outermost atomic layer. The experimentally determined energies of surface states are as follows: at point \bar{X} , 6.6 eV above E_F , designated S_0^+ ; at point \bar{Y} , 3.4 and 6.6 eV above E_F , designated S_0^+ and S_1^- , respectively.

I. INTRODUCTION

The abundance of unoccupied surface states on metals revealed recently by k -resolved inverse photoemission spectroscopy (KRIPES) raises the hope of an experimental determination of the position and shape of the surface potential barrier.¹ The observed surface states are of two kinds: the conventional Shockley surface states, and the "image states" which arise through the Coulombic asymptotic form of the surface barrier at large distances from the surface. This paper reports calculations and KRIPES measurements on Pd(110) intended to investigate further the surface barrier.

There are two reasons why Pd(110) is a promising surface on which to pursue such studies. First, the (110) surfaces of the face-centered-cubic d -band metals offer two projected bulk bands gaps: one centered at point \bar{Y} based

on the projected bulk $L_{2'}-L_1$ gap, and one at point \bar{X} based on the $X_{4'}-X_1$ gap. Both gaps support Shockley states and image states. Secondly, the upper edges (L_1 and X_1) of these gaps lie relatively high in energy for Pd, so that the entire image-state Rydberg series should reside within the gap at both \bar{Y} and \bar{X} . This is in contrast to the situation on Ni(110) or Cu(110) where the image states at \bar{Y} and \bar{X} tend to lie above the gap, becoming surface resonances degenerate with the bulk continuum.²

The relevant band energies are illustrated in Fig. 1 which shows the band structure of Pd along k_1 rods situated at the $\bar{\Gamma}$, \bar{Y} , and \bar{X} symmetry points of the surface Brillouin zone. These bands were calculated using an interpolation scheme³ fitted to the first-principles results of Christensen⁴ with some minor adjustment⁵ to improve agreement with photoemission data.⁶

II. MEASUREMENTS

The KRIPES experiments were performed in a measurement system which has been described elsewhere.⁷ The incident electrons are produced with a gun of the pervatron type⁸ whose source is an indirectly heated BaO dispenser cathode. The emitted photons are collected by an off Rowland-circle grating spectrograph using micro-channel plates to perform parallel detection over a range of photon energies. The sample was prepared by the usual cycles of ion bombardment and annealing, and its surface quality was confirmed using low-energy electron diffraction (LEED) and Auger spectroscopy.

Representative spectra are shown in Fig. 2 as a function of angle of electron incidence for the two principal azimuths $\bar{\Gamma}\bar{Y}$ and $\bar{\Gamma}\bar{X}$. These data were taken for a gun cathode voltage of 19.7 V. This corresponds to an initial energy $E_i = 22.5 \text{ eV} = 19.7 + \Phi_{\text{Pd}} - \Phi_{\text{BaO}}$ where Φ_{Pd} and Φ_{BaO} are the work functions of the sample and cathode, respectively. The spectra of Fig. 2 represent a small fraction of the data taken and were chosen to illustrate the dispersion effects for the bulk band-structure features.

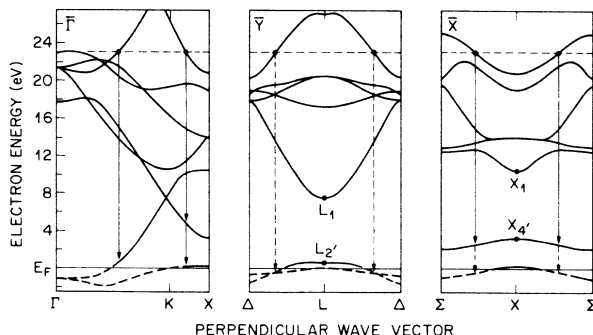


FIG. 1. Unoccupied $E(k_1)$ band structure of Pd as a function of perpendicular wave vector k_1 at the symmetry points $\bar{\Gamma}$, \bar{Y} , and \bar{X} of the (110) surface Brillouin zone. Projected gaps at \bar{Y} and \bar{X} derive from the bulk $L_{2'}-L_1$ and $X_{4'}-X_1$ gaps, respectively. Vertical arrows indicate bulk direct transitions of the kind discussed in the text.

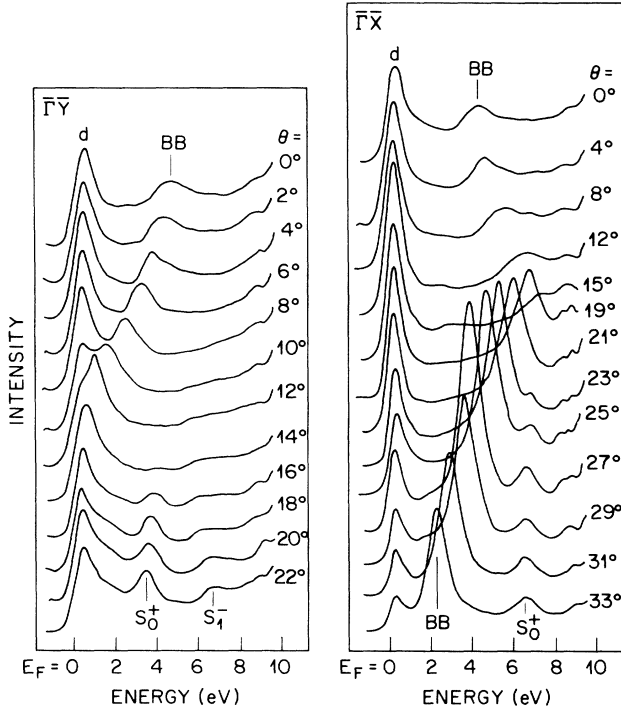


FIG. 2. KRIPES data taken on Pd(110) as a function of θ , the angle of electron incidence in the $\bar{\Gamma}\bar{Y}$ and $\bar{\Gamma}\bar{X}$ azimuths. The incident electron energy was 22.5 eV relative to E_F (gun cathode voltage of 19.7 V). Features labeled BB are attributed to direct transitions within the bulk band structure. Features labeled S_n^\pm are identified as surface states.

III. BULK BAND-STRUCTURE ANALYSIS

The bulk band structure features (designated BB) in the experimental spectra of Fig. 2 are readily explained in terms of direct transitions. The data, reduced to $E_f(k_{\parallel})$ plots in the usual way, are compared in Fig. 3 with calculated $E_f(k_{\parallel})$ plots for kinematically allowed direct transitions. The calculations were performed using an interpolation scheme.^{3,5} The initial-state energy was taken at $E_i = 23.0$ eV above E_F . The curves shown are those for which the final energy E_f lies below ~ 10 eV.

The experimental peaks identified as bulk features follow quite closely certain of the theoretical $E_f(k_{\parallel})$ curves. These are the curves for which coupling to incoming plane wave electrons is especially favorable.⁹ We attribute the small discrepancies between theory and experiment to differences in E_i (23 eV in theory, 22.5 eV in experiment) and to experimental imprecision. A very detailed comparison is possible, but has not been attempted here since our primary concern is with those features (labeled S_0^+ and S_1^- in Fig. 2) which cannot be identified with bulk band structure, and which must be due to surface states.

IV. SURFACE-STATE ANALYSIS

A. Experimental results

The KRIPES peaks identifiable as surface states may be assigned as follows. At \bar{X} we observe a surface state at

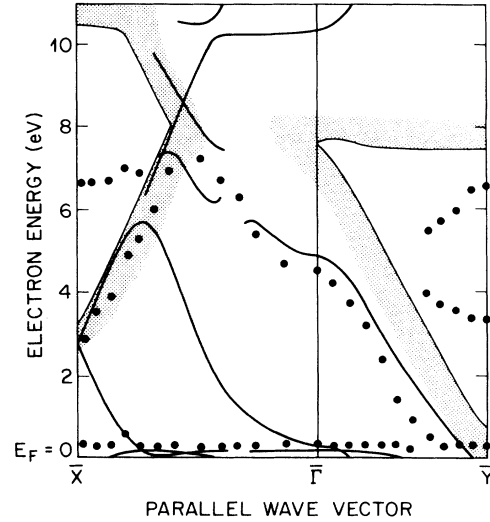


FIG. 3. $E_f(k_{\parallel})$ plot of the data of Fig. 2 (solid circles) compared with the calculated dispersion for kinematically allowed direct transitions within the bulk band structure (solid curves). The projected bulk band gaps are indicated by shading.

6.6 eV above E_F which we identify as an s_{\parallel} -like Shockley state S_0^+ . At \bar{Y} we observe two surface states: one at $E_F + 3.4$ eV identified as an S_0^+ s_{\parallel} -like Shockley state, and one at $E_F + 6.6$ eV identified as an S_1^- p_{\parallel} -like image state. The S_n^\pm classification system is described below.

B. Phase-accumulation model

We can analyze the surface-state results in terms of a simple multiple-reflection approach¹⁰⁻¹² as adapted for projected bulk band gaps centered at symmetry points on the surface Brillouin-zone boundary.² In the language of LEED theory, we have a four-beam model which can be visualized as shown in Fig. 4. In each complete cycle of multiple reflection, the surface electron approaches both the crystal barrier and the surface barrier twice. The occurrence of surface states is determined by the following quantization condition of the total phase accumulation:

$$2\phi_C + \phi_{B1} + \phi_{B2} = 2\pi n' \quad (1)$$

where n' is an integer. The phase change ϕ_C on Bragg reflection at the crystal is readily generated by a nearly-

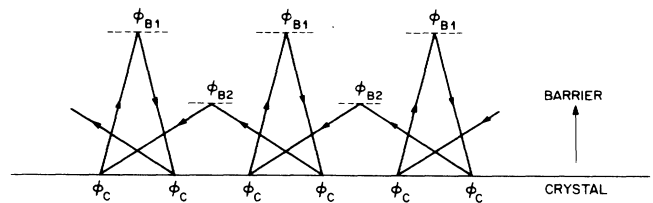


FIG. 4. Multiple-reflection model for surface state occurrence in bulk band gaps centered at the surface-Brillouin-zone boundary showing the reflection phase changes ϕ_C at the crystal, and ϕ_{B1} and ϕ_{B2} at the surface potential barrier.

free-electron model. The phase changes ϕ_{B1} and ϕ_{B2} on reflection at the surface barrier correspond, respectively, to two different values of the perpendicular momentum. These phase changes are readily computed given the shape of the surface potential barrier.

At the surface Brillouin-zone boundary, the situation is very symmetrical, and the surface states can be distinguished as odd (p_{\parallel} -like) or even (s_{\parallel} -like). This permits an alternative bookkeeping system² in which Eq. (1) is rewritten

$$\phi_C^{\pm} + \phi_B = 2\pi n, \quad (2)$$

and in which the surface states can be assigned the symbol S_n^{\pm} , where the superscript denotes even and/or odd symmetry, and the subscript, n , has the physical meaning of the number of nodes in the perpendicular component of the wave function beyond the outermost atomic layer. In this paper, we adopt the bookkeeping system of Eq. (2) and the S_n^{\pm} designations.

C. Surface potential barrier

Following a similar analysis² of Cu(110) and Ni(110), we use the surface barrier formula of Jones, Jennings, and Jepsen¹³ (referred to hereafter as the JJJ barrier). The attractive features of the JJJ barrier are its simple analytical form; the small number of adjustable parameters (z_0 , U_0 , and λ); and its resemblance in shape to first principles theoretical results.¹⁴ In Rydberg units, the JJJ barrier is expressed as

$$V_B(z) = \begin{cases} -\frac{1}{2(z-z_0)}(1 - e^{-\lambda(z-z_0)}), & z > z_0 \\ -\frac{U_0}{1 + Ae^{\beta(z-z_0)}}, & z < z_0 \end{cases} \quad (3)$$

where z_0 is the image-plane position, U_0 is the inner potential, and λ^{-1} is a characteristic distance for the changeover between the inner potential and the long-range Coulombic form of the surface barrier. The parameters A and β are fixed by the requirement of smooth continuity. The phase change, ϕ_B , at such a barrier is easily computed by integration of Schrödinger's equation along the z axis.^{2,15}

D. Comparison with experiment and discussion

Calculations of the $E(k_{\parallel})$ relations, of surface states using the phase-accumulation model are compared with experimental data in Fig. 5. For increasing n , the curves evolve from Shockley states ($n=0$) to the image-state Rydberg series ($n \geq 1$) which converges to the escape threshold (ET) given by $E_V + \hbar^2 k_{\parallel}^2 / 2m$ or $E_V + \hbar^2 (k_{\parallel}^2 - g_{\parallel}^2) / 2m$, whichever is the lowest.²

The results shown were obtained with the image-plane position z_0 placed at 2.3 a.u. beyond the outermost atom-

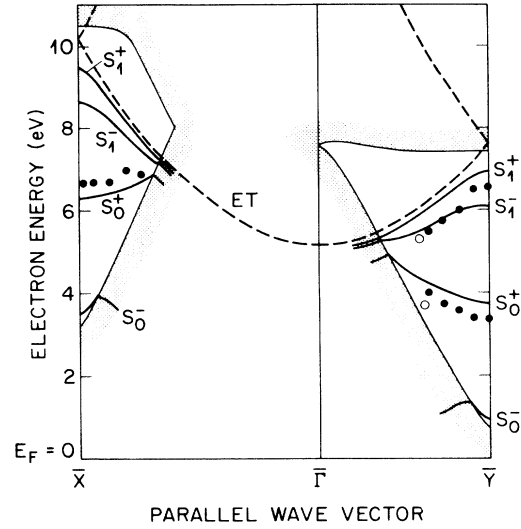


FIG. 5. $E(k_{\parallel})$ dispersion relations for surface states and image states on Pd(110). The solid curves (designated S_n^{\pm}) have been adjusted to achieve reasonable agreement with the experimental data (solid circles). Shading indicates the projected continuum of bulk states. The dashed curve (ET) is the electron escape threshold.

ic layer. This value is essentially the same as the 2.4-a.u. distance found for Ni(110) and Cu(110) also using the JJJ barrier.² The internal precision of the fit for z_0 is $\sim \pm 0.2$ a.u. It must be stressed that the derived values for z_0 are prejudiced by the choice of surface barrier formula. Had we used the alternative and equally plausible formula of Rundgren and Malström,¹⁶ we would have arrived at a value for z_0 smaller by ~ 1 a.u.

We were unable in this work to observe the lowest lying Shockley surface state (S_0^- in our terminology) either at \bar{X} or \bar{Y} . These are presumably surface resonances existing below the bottom of the respective band gaps, and may succumb to future investigations. Nor were we able to detect the first S_1^- image state at \bar{X} . Higher lying image states S_2^{\pm} etc. were not detected. Thus our original hope of using the specific surface Pd(110) to display the full panoply of Shockley states and image states has not been realized. The S_0^+ states have been observed at both \bar{X} and \bar{Y} , and the S_1^- state has been observed at \bar{Y} . The latter state is especially important since it is an image state; that is to say it is a state which arises from the Coulombic asymptotic form for the surface barrier. Thus we are able to make some useful statements on the position of the image plane.

ACKNOWLEDGMENTS

This work was supported in part by U. S. Department of Energy, Contract No. DE-AC02-76CH00016.

¹N. V. Smith and D. P. Woodruff, Prog. Surf. Sci. **21**, 295 (1986), and references therein.

²C. T. Chen and N. V. Smith, Phys. Rev. B **35**, 5407 (1987).

³N. V. Smith, Phys. Rev. B **19**, 5019 (1979).

⁴N. E. Christensen, Phys. Rev. B **14**, 3446 (1976).

⁵D. A. Wesner, P. D. Johnson, and N. V. Smith, Phys. Rev. B **30**, 503 (1984).

⁶F. J. Himpsel and D. E. Eastman, Phys. Rev. B **18**, 5236 (1978).

- ⁷P. D. Johnson, S. L. Hulbert, R. F. Garrett, and M. R. Howells, *Rev. Sci. Instrum.* **57**, 1324 (1986).
- ⁸N. G. Stoffel and P. D. Johnson, *Nucl. Instrum. Methods A* **234**, 230 (1985).
- ⁹D. P. Woodruff, N. V. Smith, P. D. Johnson and W. A. Royer, *Phys. Rev. B* **26**, 2943 (1982); R. F. Garrett and N. V. Smith *ibid.* **33**, 3740 (1986).
- ¹⁰P. M. Echenique and J. B. Pendry, *J. Phys. C* **11**, 2065 (1978).
- ¹¹E. G. McRae, *Surf. Sci.* **25**, 491 (1971); *Rev. Mod. Phys.* **51**, 541 (1979).
- ¹²N. V. Smith, *Phys. Rev. B* **32**, 3549 (1985).
- ¹³R. O. Jones, P. J. Jennings, and O. Jepsen, *Phys. Rev. B* **29**, 6474 (1984).
- ¹⁴N. D. Lang and W. Kohn, *Phys. Rev. B* **1**, 4555 (1970); **7**, 3541 (1973).
- ¹⁵E. G. McRae and M. L. Kane, *Surf. Sci.* **108**, 435 (1981).
- ¹⁶J. Rundgren and G. Malström, *J. Phys. C* **10**, 4671 (1977).

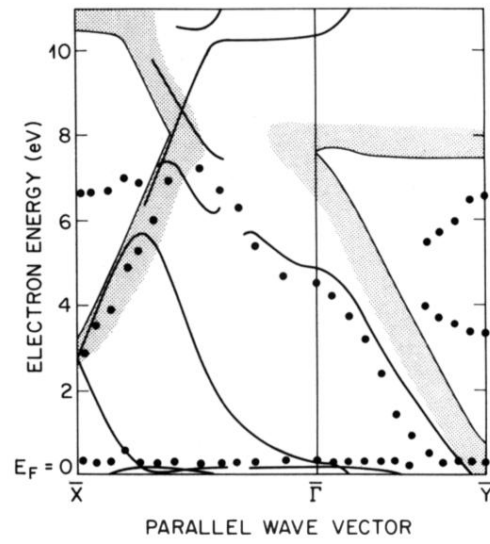


FIG. 3. $E_f(k_{\parallel})$ plot of the data of Fig. 2 (solid circles) compared with the calculated dispersion for kinematically allowed direct transitions within the bulk band structure (solid curves). The projected bulk band gaps are indicated by shading.

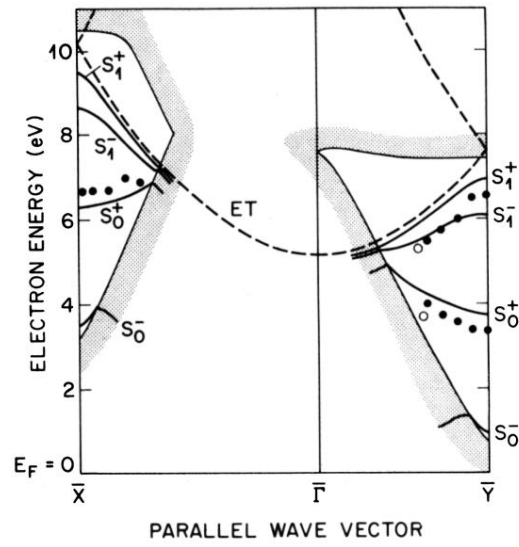


FIG. 5. $E(k_{\parallel})$ dispersion relations for surface states and image states on Pd(110). The solid curves (designated S_n^{\pm}) have been adjusted to achieve reasonable agreement with the experimental data (solid circles). Shading indicates the projected continuum of bulk states. The dashed curve (ET) is the electron escape threshold.